Journal Name

Dynamic Article Links ▶

ARTICLE TYPE

Fluorescent Molecular Rotors Based on the BODIPY Motif: Effect of Remote Substituents

Effat Bahaidarah,[a] Anthony Harriman,*[a] Patrycja Stachelek , [a] Sandra Rihn,[‡b] Elodie Heyer[b] and Raymond Ziessel[b]

The ability of an unconstrained boron dipyrromethene dye to report on changes in local viscosity is improved by appending a single aryl ring at the lower rim of the dipyrrin core. Recovering the symmetry by attaching an identical aryl ring on the opposite side of the lower rim greatly diminishes the sensory
10 activity, as does blocking rotation of the meso-aryl group. On the basis of viscosity- and temperature-dependence studies, together with quantum chemical calculations, it is proposed that a single aryl ring at the 3-position extends the molecular surface area that undergoes structural distortion during internal rotation. The substitution pattern at the lower rim also affects the harmonic frequencies at the bottom of the potential well and at the top of the barrier. These effects can be correlated with the separation of the
15 H_1, H_7 hydrogen atoms.

Introduction

A substantial body of information has accumulated regarding small molecules whose fluorescence properties are controlled, at least to some degree, by the extent of frictional forces between
20 the molecule (i.e., the rotor) and the surrounding environment. Such systems, which should be distinguished from cases where intramolecular charge transfer causes minor structural change, can be used to probe the local rheology and to operate as crude temperature or pressure indicators.[1] Related systems form the
25 basis of molecular machines,[2] switches,[3] sensors,[4] etc. and there is a steadily growing interest in applying molecular rotors to monitor changes in viscosity within biological media[5] or nano-cavities.[6,7] Of the known molecular systems that function as fluorescent rotors, the boron dipyrromethene (BODIPY) family
30 of dyes[8] has many important advantages and has been used as the starting point for the design of several different types of rheology probes.[9-16]

As reported first by Holten et al.[17] these BODIPY-based rotors operate by partial restriction of the rotation of a meso-phenylene
35 ring around a relatively unconstrained dipyrrin backbone. Such rotation by itself will not affect the emissive properties of the BODIPY nucleus but, in order for the phenylene ring to complete a full turn, it is necessary for the dipyrrin backbone to buckle slightly. It is this latter process that leads[10,17] to enhanced
40 nonradiative decay. The underlying structural change creates the possibility to correlate fluorescence intensity with key properties of the local environment. Attaching bulky substituents to either the phenylene ring[11] or the 1,7-positions of the dipyrrin backbone[10,17] affects the rotary action, in many cases curtailing
45 the sensory capability. We now show that gross modulation of the rotor-like behaviour can be realized by attaching aryl groups at

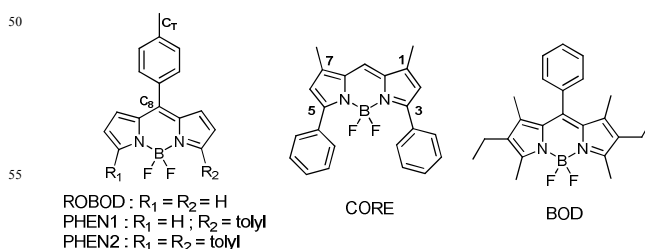the lower rim of the BODIPY unit, well away from the buckling dipyrrin core.

Figure 1. Molecular formulae of the compounds investigated herein.

60 Results and Discussion

Molecular structures for the target compounds are shown by way of Figure 1 and are based on the unconstrained[17] BODIPY nucleus. The prototypic fluorescent rotor, ROBOD, has been studied previously[10,13] and is used here as a reference compound.
65 Likewise, the constrained analogue, BOD, bearing methyl groups at the 1,7-positions, has received extensive study in the literature.[8] This highly fluorescent dye cannot be applied to monitor changes in the local environment. Simple derivatives of ROBOD are PHEN1 and PHEN2, which are equipped with one
70 or two tolyl groups at positions where they will not block rotation of the *meso*-substituent by steric factors. The series is augment by a control compound, CORE, which has the ancillary tolyl groups at the 3,5-positions but lacks the *meso*-phenyl group. It might be noted that the alkyl groups present in certain derivatives affect the
75 absorption and emission spectral properties by way of inductive effects.[8] The synthesis of the new dyes was inspired by previously described[18,19] protocols as outlined in the Supporting

Information.

Table 1. Summary of the photophysical properties recorded for the target compounds in MTHF at 20 ^{0}C.

Property	ROBOD	BOD	PHEN1	PHEN2	CORE
λ_{MAX} / nm	502	525	531	559	547
ε_{MAX} / M^{-1}cm^{-1}	71,000	74,000	59,100	62,235	62,100
λ_{FLU} / nm	530	547	564	602	588
SS / cm^{-1}	1,050	765	1,105	1,280	1,280
Φ_F	0.023	0.78	0.013	0.28	0.92
τ_S / ns	0.15	5.4	0.092	2.1	6.6
k_{RAD} / 10^8 s^{-1}	1.50	1.45	1.42	1.30	1.40
k_{NR} / 10^8 s^{-1}	65	0.40	110	3.5	0.12

(a) absorption maximum; (b) molar absorption coefficient; (c) emission maximum; (d) Stokes' shift; (e) fluorescence quantum yield; (f) excited-singlet state lifetime; (g) radiative rate constant; (h) non-radiative rate constant for decay of the S_1 state.

The photophysical properties of ROBOD were recorded in 2-methyltetrahydrofuran (MTHF) at room temperature and the main findings are collected in Table 1; N.B. the same properties recorded in dichloromethane at room temperature are reported in Table S1 (see Electronic Supporting Information). The absorption maximum (λ_{MAX}) occurs at 502 nm, with a molar absorption coefficient (ε_{MAX}) of 71,000 M^{-1} cm^{-1}. There is a modest Stokes' shift (SS = 1,050 cm^{-1}), with the fluorescence maximum (λ_{FLU}) lying at 530 nm. The emission profile shows reasonable mirror symmetry with the absorption spectrum and there is excellent correspondence between absorption and excitation spectra (Figure S1). Similar behaviour is found for the constrained analogue BOD, allowing for a 20-nm red shift induced by the alkyl substituents (Table 1). The two compounds exhibit rather disparate fluorescence quantum yields (Φ_F) and excited-state lifetimes (τ_S) under these conditions, with ROBOD being weakly emissive. Radiative rate constants (k_{RAD}), which remain in good agreement with those calculated from the Strickler-Berg expression,[20] are comparable while the corresponding nonradiative rate constants (k_{NR}) reflect the difference in emission yields (Table 1). We attribute the fast deactivation of the excited-singlet state of ROBOD to the internal rotor effect, as has been done previously[10,17] and which for BOD is inhibited by the presence of the 1,7-methyl groups. We return later to the exact meaning of this phenomenon: Firstly, we consider the effects of substitution at the lower rim of the BODIPY nucleus.

Insertion of a tolyl group at the 3-position introduces a 30-nm red shift for both absorption and emission spectra relative to ROBOD (Figure S2), while there is a small (i.e., 10%) increase in the magnitude of the Stokes' shift. Also, the absorption band is somewhat broader for PHEN1 compared to ROBOD, reflecting a certain degree of heterogeneity for the ground-state geometry that largely disappears on excitation. More importantly, there is a

significant fall in both Φ_F and τ_S without perturbing k_{RAD}. The decreased fluorescence, therefore, is a consequence of an enhancement in k_{NR}. Appending a second tolyl ring at the 5-position, forming PHEN2, leads to a dramatic increase in both Φ_F and τ_S. At the same time, such substitution increases the Stokes' shift, further broadens the absorption spectral profile, amplifies the red shifts to >60 nm and partially assuages k_{NR}. Moving to the control molecule lacking the *meso*-substituent, CORE, we find that Φ_F and τ_S exceed those found for BOD, although there is an exacerbated red shift and broadening of the absorption profile. Throughout this series there is a progressive decrease in k_{RAD} as the emission peak moves towards lower energy, as is to be expected from the Strickler-Berg expression.[20] The red shifts are probably due to increased π-conjugation caused by partial orbital mixing between dipyrrin and tolyl substituent. Indeed, this assertion is supported by the results of DFT (B3LYP/6-31+G(d)/PCM) calculations that indicate orbital mixing for the LUMO but not for the corresponding HOMO (see ESI). Comparison of the photophysical properties recorded for the unconstrained dyes with those found for the control compounds indicates that nonradiative decay is promoted by the presence of a *meso*-aryl ring.
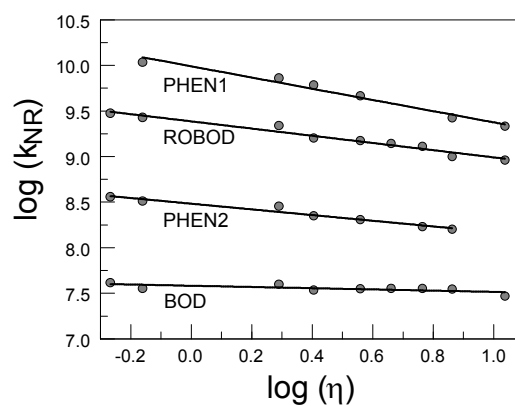

Figure 2. Effect of solvent viscosity on the rate constant for nonradiative decay measured in a series of linear alcohols at 20 ^{0}C.

$$k_{NR} = \frac{\nu}{\eta^{\alpha}} \exp\left(-\frac{E_A}{RT}\right) \quad (1)$$

Increasing solvent viscosity (η), by using a homologous series of n-alcohols at 20 ^{0}C, leads to a progressive increase in τ_S for ROBOD, PHEN1 and PHEN2 but not for CORE, thereby confirming that each of these unconstrained molecules operates as a fluorescent rotor. Across this series of solvents, there is a reasonably linear relationship between k_{NR} and shear viscosity, as considered in the form of log-log plots (Figure 2), but with differing gradients and intercepts. Indeed, the experimental data collected at 20 ^{0}C can be considered in terms of Equation 1,[21] where ν corresponds to a limiting pressure exerted by the rotor, α is a coefficient that effectively describes the sensitivity towards viscosity, and E_A is a barrier for internal rotation (Table 2). For the prototypic rotor ROBOD, α has a value of 0.41, which is

similar to that determined earlier for a closely related dye,[10] and this falls to 0.31 for PHEN2. In contrast, α determined for PHEN1 is 0.62, which is the highest such value found for any BODIPY-based rotor and is far superior to that measured for the industry standard[22] under the same conditions. Thus, PHEN1 performs remarkably well as a fluorescent rotor, in marked contrast to PHEN2. Of the two control compounds, CORE shows no viscosity dependence while BOD exhibits a shallow (α ≈ 0.07), but definite, sensitivity towards shear viscosity (Figure 2).

In separate experiments, Φ_F was examined as a function of temperature in MTHF. After correction[23] for solvent contraction on cooling, Φ_F for CORE is barely affected by changes in temperature whereas that for BOD is constant at temperatures below 200K but decreases steadily, albeit marginally, as the temperature is raised further (Figure S3). Neither of these compounds functions as a viable molecular rotor. In marked contrast, Φ_F for ROBOD increases progressively with decreasing temperature until approaching the freezing point (T_F = 137 K) of the solvent. As the solvent solidifies, Φ_F increases dramatically before remaining essentially constant in both amorphous (Φ_F = 0.93) and glassy (Φ_F = 0.99) regions; note that the limiting Φ_F measured in the glassy matrix is comparable to that of CORE under these conditions. This behaviour, which amounts to a 45-fold variation in Φ_F over the full temperature range, is considered typical for a fluorescent rotor. Both PHEN1 and PHEN2 show similar temperature-dependent Φ_F to that observed for ROBOD (Figure S3), confirming that these compounds operate as fluorescent rotors. The total variation in Φ_F found for PHEN2 is only ca. 3-fold, but that for PHEN1 varies by a factor of ca. 75-fold and is far greater than that recorded for ROBOD. For each compound, Φ_F approaches unity in the glassy matrix.

Small spectral shifts accompany the freezing and vitrification processes, as is exemplified for PHEN2 in Figure S4, although the absorption and emission maxima do not correlate with changes in solvent polarisability. Here, the emission maximum moves towards lower energy as the temperature falls throughout the liquid phase, amounting to a red shift of ca. 200 cm^{-1} between 290 and 150 K, before shifting slightly to higher energy as the solvent freezes. The initial red shift can be explained in terms of increased π-electron delocalization between dipyrrin and the 3,5-tolyl rings; identical behaviour is found with both CORE and PHEN1 but not for either BOD or ROBOD. The core aryl ring(s) has a dihedral angle of ca. 50[0] (B3LYP/6-31+G(d)/PCM) for all three derivatives but rotation at the connecting C-C linkage is facile except at around 20[0] where some instability is caused by close proximity (i.e., 1.6 Å) between a fluorine atom and the *ortho*-hydrogen atom on the tolyl ring. This steric clash introduces a barrier (i.e., 50 kJ/mol) for complete rotation of the core-tolyl ring but there are wide ranges over which oscillation is essentially barrierless. Each of these compounds can attain the geometry having the core-tolyl ring aligned with the dipyrrin unit (Figure S5). This alignment will maximize π-conjugation, leading to the observed red-shifted absorption and emission spectra, as confirmed by molecular orbital calculations (Figure S6). A significant feature of these calculations is that planarization of the core tolyl rings causes the dipyrrin unit to display slight curvature. It is also apparent that excitation favours adoption of a conformation where the core aryl rings are more aligned with the

dipyrrin unit and with the latter being somewhat more curved (see ESI).

$$k_{NR} = k_0 + k_{ACT} \exp\left(-\frac{E_A}{R[T - T_G]}\right) \qquad (2)$$

For CORE, the nonradiative decay rate constant, k_{NR}, is independent of temperature throughout the range where the solvent is fluid (T >140K). For each of the other compounds, the effect of temperature on k_{NR} can be satisfactorily explained in terms of Equation 2 (Figure 3) where k_0 refers to an activationless rate constant, k_{ACT} is the corresponding activated term and T_G (= 110K) is the glass transition temperature of MTHF (Table 2). The activation barrier, E_A, contains contributions from both changes in viscosity and internal rotation. The activationless rates are relatively slow and fall into two distinct groups; those pertaining to the effective rotors ($k_0 > 10^8$ s[-1]) and those associated with poor rotors ($k_0 = 10^7$ s[-1]). The activated terms are sensitive towards substitution pattern and vary dramatically among the various compounds.
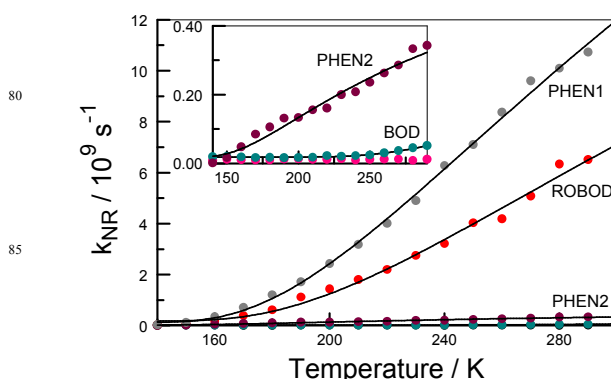

Figure 3. Effect of temperature on the derived rate constants for nonradiative decay as recorded in MTHF: PHEN1 (grey points), ROBOD (red points), PHEN2 (plum points), BOD (blue points) and CORE (crimson points). Solid lines refer to nonlinear-least square fits to Equation 2. The insert shows an expansion of the low-temperature region. For convenience, the experimental data are given in the Supporting Information.

There is a comparatively large barrier for BOD that can only be crossed at elevated temperature. For the remaining compounds, the magnitude of the barrier decreases with increasing effective mass of the dipyrrin unit. As mentioned above, the core tolyl groups cause slight curvature of this latter unit, which escalates as the two groups become co-planar. Double substitution, and also electronic excitation, increases this curvature and forces the *meso*-aryl ring out of the plane of symmetry, as is evident by the B-C_8-C_T angle[24] (Table 2). Forced curvature of the dipyrrin backbone also introduces asymmetry for the two fluorine atoms and this is a convenient tool by which to represent geometric perturbation (Table 2). At the excited-state level, this structural distortion will rupture the S_1 surface so as to create pinholes[25] (or conical intersections[26]) through which the wave-packet can escape back to the ground state. Within this model, it is entirely intuitive that E_A is controlled, in part, by the difference in initial geometry of the reactant and that at the pinhole. This pinhole is not the transition state for full rotation of

the *meso*-aryl ring and, as a consequence, is rather difficult to characterise.

Table 2. Compilation of the various parameters associated with rotation of the *meso*-aryl ring.

Property	ROBOD	BOD	PHEN1	PHEN2	CORE
$k_0 / 10^7 s^{-1}$ (a)	17	1.8	12	1.9	1.2
$k_{ACT} / 10^9 s^{-1}$ (b)	36.5	5.9	51.0	0.8	NA
E_A /kJ mol^{-1} (c)	2.6	7.7	2.3	1.4	NA
α (d)	0.41	0.07	0.62	0.31	NA
B-C$_8$-C$_T$ / ^{0} (e)	179.8	180.0	178.8	177.9	NA
B-C$_8$-C$_T$ / ^{0} (f)	177.8	179.8	176.3	175.2	NA
B-C$_8$-C$_T$ / ^{0} (g)	163.5	146.6	163.4	162.1	NA
A$_{F,F}$ / ^{0} (e)	0.12	0.04	4.4	6.9	5.1
A$_{F,F}$ / ^{0} (f)	1.2	0.27	5.4	9.5	5.5
A$_{F,F}$ / ^{0} (g)	28.5	30.0	30.4	32.0	NA
H$_1$H$_7$ / Å (f)	5.670	5.279	5.717	5.518	5.700

(a) Activationless rate constant according to Equation 2. (b) Activated rate constant according to Equation 2. (c) Activation energy according to Equation 2. (d) Viscosity sensitive parameter according to Equation 2. (e) Refers to the ground state. For atom labeling see Figure 1. (f) Refers to the first-allowed excited state. (g) Refers to the transition state for full rotation of the *meso*-aryl ring.

Several parameters combine to define the performance of the dye in terms of its ability to function as a fluorescent rotor, including α, k_{ACT} and k_0. The relative values determined for α can be considered as a crude measure of the volume of solvent affected by the geometry change undertaken by the solute. For BOD, few solvent molecules are affected and the geometry change is considered to be either minor or highly localised. Symmetrical dyes, such as ROBOD and PHEN2, are susceptible to buckling of the dipyyrin core, but according to semi-empirical (PM6, RHF, COSMO) quantum chemical calculations this is mostly restricted to the upper rim. Asymmetrical dyes, such as PHEN1, undergo more substantive structural distortion during rotation and this will engage more solvent molecules. We now see a clear correlation between α and the asymmetry factor A$_{F,F}$,[27] the latter being a convenient monitor of the extent of structural change needed to effect full rotation. Since the computed rotational barriers are much less than those derived experimentally for the excited-singlet state, it should be considered that full rotation is not a pre-requisite for sensing activity.

The derived k_0 values are thought to describe the harmonic frequency at the bottom of the potential well[28] where the friction coefficient might be large. The results indicate a substantial increase in this frequency for ROBOD and PHEN1 relative to the more constrained analogues. This constraint is imposed by the blocking methyl groups present in BOD and by the pincher effect of the core-phenylene rings for PHEN2 that force the H$_1$,H$_7$ atoms into closer proximity. In fact, there is a crude correlation between k_0 and the H$_1$,H$_7$ distance computed for the excited-singlet state. Likewise, the derived k_{ACT} values can be considered

to represent, at least in part, the harmonic frequency at the top of the barrier[28] and, as such, are associated with the corresponding escape rates at the pinhole. It appears that k_0 and k_{ACT} are correlated and, on this basis, we can infer that the same structural facets, most notably the extent of H$_1$,H$_7$ separation, control both frequencies. Clearly, retaining high symmetry does not facilitate development of improved molecular rotors.

Conclusions

The development of fluorescent probes for in situ monitoring of changes in rheology is an active research field with important applications in medicine, chemical engineering, environmental preservation and personal security. Advanced molecular sensors are required that display highly selective properties and this need creates the stimulus for the design of novel reagents that advance the state-of-the-art. Probes based on the BODIPY fluorophore are attractive reagents because of their robustness, high radiative rate constants and facile modification by synthetic procedures. The results outlined above indicate that improved performance might be achieved by incorporating substituents at remote sites on the BODIPY fluorophore. Aryl substituents attached at the lower rim of the dipyrrin unit serve to push the absorption and emission maxima towards the red region, via increased π-conjugation, and to squeeze the upper rim by what might be termed "a scissor-like effect". The latter situation affects the space available for the meso-aryl rotor and modulates the rate of nonradiative decay of the fluorescent state. The disparity between symmetrical and asymmetrical derivatives is most unexpected and clearly opens the way to design new and improved sensors.

Acknowledgements

Notes and references

^{a} Molecular Photonics Laboratory, School of Chemistry, Bedson Building, Newcastle University, Newcastle upon Tyne, NE1 7RU, United Kingdom. Fax: 44 191 208 8660; Tel: 44 191 208 8660; E-mail: anthony.harriman@ncl.ac.uk
^{b} Laboratoire de Chimie Organique et de Spectroscopies Avancées (ICPEES-LCOSA), UMR 7515 CNRS, 25 rue Becquerel, 67087 Strasbourg Cedex 2, France.
† Electronic Supplementary Information (ESI) available: Synthesis and characterization of PHEN1, PHEN2 and CORE, experimental and computational details, additional spectroscopic data, effect of temperature on Φ$_F$ and output from the quantum chemical calculations.
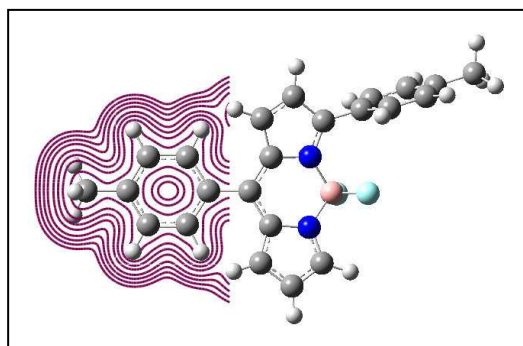‡ Present address: School of Chemistry, Bedson Building, Newcastle University, Newcastle upon Tyne, NE1 7RU, United Kingdom.

REFERENCES

1. M. A. Haidekker and E. A. Theodorakis, Environment-sensitive Behavior of Fluorescent Molecular Rotors. *J. Biol. Engineer*. **2010**, *4*, 11-25.
2. W. R. Browne and B. L. Feringa, Making Molecular Machines Work. *Nature Technol*. **2006**, *1*, 25-35.
3. N. Koumura, R. W. J. Nijlstra, R. A. van Delden, N. Harada and B. L. Feringa, Light-driven Monodirectional Molecular Rotors. *Nature* **1999**, *401*, 152-155.

4. M. A. Haidekker, W. Akers, D. Lichlyter, T. P. Brady and E. A. Theodorakis, Sensing of Flow and Shear Stress using Fluorescent Molecular Rotors. *Sensor Lett.* **2005**, *3*, 42-48.

5. R. M. Yusop, A. Unciti-Broceta and M. Bradley, A Highly Sensitive Fluorescent Viscosity Sensor. *Biorg. Med. Chem. Lett.* **2012**, *22*, 5780-5783.

6. K. Gawala, W. D. Sasikala, A. Sengupta, S. A. Dalvi, A. Mukherjee and P. Hazra, Modulation of Excimer Formation of 9-(Dicyanovinyl)-Julolidene by the Macroscopic Host. *Phys. Chem. Chem. Phys.* **2013**, *15*, 330-340.

7. M. D'Amico, G. Schiro, A. Cupane, L. D'Alfonso, M. Leone, V. Militello and V. Vetri, High Fluorescence of Thioflavin T Confined in Mesoporous Silica Xerogels. *Langmuir* **2013**, *29*, 10238-10246.

8. G. Ulrich, R. Ziessel and A. Harriman, The Chemistry of Fluorescent BODIPY Dyes: Versatility Unsurpassed. *Angew. Chem., Int. Ed.* **2008**, *47*, 1184-1201.

9. M. K. Kuimova, G. Yahioglu, J. A. Levitt and K. Suhling, Molecular Rotor Measures Viscosity of Live Cells via Fluorescence Lifetime Imaging. *J. Am. Chem. Soc.* **2008**, *130*, 6672-6673.

10. M. A. H. Alamiry, A. C. Benniston, G. Copley, K. J. Elliott, A. Harriman, B. Stewart and Y.-G. Zhi, A Molecular Rotor Based on an Unhindered Boron Dipyrromethene (Bodipy) Dye. *Chem. Mater.* **2008**, *20*, 4024-4032.

11. J. A. Levitt, M. K. Kuimova, G. Yahioglu, P.-H. Chung, K. Suhling and D. Phillips, Membrane-bound Molecular Rotors Measure Viscosity in Live Cells via Fluorescence Lifetime Imaging. *J. Phys. Chem. C* **2009**, *113*, 11634-11642.

12. A. C. Benniston, A. Harriman, V. L Whittle and M. Zelzer, Molecular Rotors Based on the Boron Dipyrromethene Fluorophore. *Eur. J. Org. Chem.* **2010**, 523-530.

13. M. A. H. Alamiry, E. Bahaidarah, A. Harriman, T. Bura and R. Ziessel, Fluorescent Molecular Rotors under Pressure: Synergistic Effects of an Inert Polymer. *RSC Advances* **2012**, *2*, 9851-9859.

14. N. A. Hosny, G. Mohamedi, P. Rademeyer, J. Owen, Y. Wu, M.-X. Tang, R. J. Eckersley, E. Stride and M. K. Kuimova, Mapping Microbubble Viscosity using Fluorescence Lifetime Imaging of Molecular Rotors. *Proc. Natl. Acad. Sci. USA* **2013**, *110*, 9225-9230.

15. P. Loison, N. A. Hosny, P. Gervais, D. Champion, M. K. Kuimova and J.-M. Perrier-Cornet, Direct Investigation of Viscosity of an Atypical Inner Membrane of Bacillus Spores: A molecular Rotor/FLIM Study. *Biochim. Biophys. Acta* **2013**, *1828*, 2436-2443.

16. H. Zhu, J. Fan, M. Li, J. Cao, J. Wang and X. Peng A "Distorted-BODIPY"-based Fluorescent Probe for Imaging of Cellular Viscosity in Live Cells. *Chem. Eur. J.* **2014**, *20*, 4691-4696.

17. H. L. Kee, C. Kirmaier, L. Yu, P. Thamyongkit, W. J. Youngblood, M. E. Calder, L. Ramos, B. C. Noll, D. F. Bocian, W. R. Scheidt, R. R. Birge, J. S. Lindsey and D. Holten, Structural Control of the Photodynamics of Boron-Dipyrrin Complexes. *J. Phys. Chem. B* **2005**, *109*, 20433-20443.

18. S. Rihn, P. Retailleau, N. Bugsaliewicz, A. De Nicola and R. Ziessel, Versatile Synthetic Methods for the Engineering of Thiophene-Substituted BODIPY Dyes. *Tetrahedron Lett.* **2009**, *50*, 7008-7013.

19. A. Poirel, A. De Nicola, P. Retailleau and R. Ziessel, Oxidative Coupling of 1,7,8-Unsubstituted BODIPYs: Synthesis and Electrochemical and Spectroscopic Properties. *J. Org. Chem.* **2012**, *77*, 7512-7525.

20. S. J. Strickler and R. A. Berg, Relationship between Absorption Intensity and Fluorescence Lifetime of Molecules. *J. Chem. Phys.* **1962**, *37*, 814-822.

21. S. P. Velsko and G. R. Fleming, Solvent Influence on Photochemical Isomerizations – Photophysics of DODCI. *Chem. Phys.* **1982**, *65*, 59-70.

22. B. D. Allen, A. C. Benniston, A. Harriman, S. A. Rostron and C. F. Yu, The Photophysical Properties of a Julolidene-based Molecular Rotor. *Phys. Chem. Chem. Phys.* **2005**, *7*, 3035-3040.

23. P. D. Zoon and A. M. Brouwer, A Push-Pull Aromatic Chromophore with a Touch of Merocyanine. *Photochem. Photobiol. Sci.* **2009**, *8*, 345-353.

24. The term B-C8-CT refers to the angle tended by the boron atom, the meso-carbon atom and the carbon atom of the para-methyl group on the tolyl group (for BOD this latter atom is replaced with the para-hydrogen atom).

25. D. Ben-Motz and C. B. Harris, Torsional Dynamics of Molecules on Barrierless Potentials in Liquids. II. Test of Theoretical Models. *J. Chem. Phys.* **1987**, *86*, 5433-5440.

26. B. G. Levine and T. J. Martinez, Isomerization Through Conical Intersections. *Ann. Rev. Phys. Chem.* **2007**, *58*, 613-634.

27. Calculated as the difference between the two C8-B-F bond angles.

28. S. P. Velsko, D. H. Waldeck and G. R. Fleming, Breakdown of Kramers Theory Description of Photochemical Isomerization and the Possible Involvement of Frequency Dependent Friction. *J. Chem. Phys.* **1983**, *78*, 249-258.

Table of Contents Entry